JOURNAL OF APPLIED ELECTROCHEMISTRY 11 (1981) 613–623

Impedance measurements during the cycling of a zinc electrode

C. CACHET, U. STRÖDER, R. WIART

Groupe de Recherche No. 4 du CNRS 'Physique des Liquides et Electrochimie', associé à l'Université Pierre et Marie Curie, 4 place Jussieu, 75230 Paris Cedex 05, France

Received 19 November 1980

Impedance spectra have been obtained during the cycling of a zinc electrode both in a Leclanché-cell-type electrolyte and in an alkaline zincate solution. Changes in impedance plots indicate an increase in the electrode area and a variation of the electrode kinetics with cycling. The kinetics of zinc deposition appear to be very sensitive to the contamination of electrolytes by dissolution products. The results confirm a correlation between the presence of an additive such as NBu_4Br and the increase of the cycle life of the zinc electrode.

1. Introduction

It is known that impedance measurements carried out over a wide range of frequencies have particular relevance to the investigation of electrode reactions. The method has been extensively applied in our laboratory to the study of the mechanism of zinc deposition [1–4] and zinc dissolution [5, 6] in the various media used in commercial battery devices.

Impedance measurements at very low frequencies have allowed the detection of interfacial processes not accessible by polarization curves. The experimental results obtained by this method have led us to describe zinc electrodeposition [2] and zinc electrodissolution [7] by models of interfacial reactions, establishing close correlations between the electrode kinetics and the electrode morphology. Modifications to the electrode kinetics, observed when inhibitors of dendritic growth are present in the electrolyte, have provided information on the mechanism of the inhibition of the irregular growth and dissolution of zinc [3–6].

Recently, impedance measurements have been proposed as an efficient state-of-charge test for batteries [8] and the frequency response of Leclanché cells in various states of charge has been investigated by this technique [9]. The results have suggested a device based on the response of the cell at an appropriate frequency [10] for the rapid testing of cell quality. Previously [11, 12], measurements of the double-layer capacitance of zinc electrodes performed in the presence of inhibitors had suggested that this method might serve as a useful tool in selecting substances which would be most effective in extending the cycle life of the zinc electrode.

In this paper, we show that impedance measurements also present a nondestructive and convenient *in situ* method for following the zinc electrode behaviour during charge and discharge cycles. The kinetics of the cycled electrode are studied in acidic and alkaline electrolytes commonly used for industrial purposes in electrochemical cells. With this experimental approach we show that organic additives like tetrabutylammonium bromide (NBu_4Br) improve the life of rechargeable zinc electrodes. Measurements were carried out under conditions of forced convection in order to control electrochemical steps involving the transport of reactants. The influence of cycling on the electrode morphology was studied by scanning electron microscopy.

2. Experimental

In order to conduct this present study, we have chosen two types of electrolytes commonly used in the zinc industry. One (2.67 M NH_4Cl +

0021–891X/81/050613–11$03.10/0

0.72 M $ZnCl_2$) was a Leclanché cell electrolyte, the pH of which was adjusted to 5.2 by adding NH_4OH. The second electrolyte was an alkaline medium (5 M KOH + 0.5 M ZnO) employed in accumulators. All the solutions were prepared with doubly ion-exchanged water, passed through a carbon cartridge and a micropore filter, and then twice distilled in a quartz apparatus. The salts were 'Merck' compounds of analytical purity, and high-purity NBu_4Br (Fluka) was used. During the electrolysis, the solution was maintained at 26 ± 0.5° C. The atmosphere in the cell was argon. The counter electrode was made of either a platinum-gauze cylinder, or a sheet of high-purity zinc (Koch-Light Laboratories, 99.999%). The reference electrode immersed in the electrolyte had two compartments separated by fritted-glass and was filled with a saturated KCl solution. The working electrode was a cut from a zinc cylinder (Johnson Matthey, 99.999%) of 0.2 cm^2 area whose lateral wall was insulated by a thermoretractable plastic tube. The electrode was a rotating disc whose speed could be altered from 0 to 5000 r.p.m. The rotation speed was chosen to be sufficiently high to avoid any influence on the observed phenomena. Before each experiment the electrode surface was polished by emery paper (600 grade), then immersed into a 37% HCl solution for a few seconds and rinsed.

Impedance measurements were carried out galvanostatically as previously described [13]. Operating conditions of 5, 10 and 25 mA cm^{-2} were used for most of the experiments. The direct current was reversed manually by adjusting the pilot voltage of the galvanostat, except for cycles carried out during several days, in which case the cell was automatically cycled using a square waveform generator delivering a given current through a resistance at a fixed frequency. The surface morphology of the electrodes after total electrolysis was examined by scanning electron microscopy (SEM).

3. Results and discussion

3.1. *Zinc electrode cycled in a Leclanché cell electrolyte*

Experimental results obtained with a zinc electrode cycled in the Leclanché cell electrolyte and using a zinc counter electrode are illustrated in Fig. 1. Alternate deposition (Diagrams 1–5) and dissolution (Diagrams 1′–4′) were performed at 25 mA cm^{-2} for 30 min. Under these conditions the thickness of zinc deposited and dissolved during each cycle was 21 μm. With an electrode rotated at 2600 r.p.m. no Warburg component appears on the impedance diagrams. As previously shown [1], Diagram 1 reveals a capacitive loop between 60 kHz and 140 Hz corresponding to the double-layer capacity (80 $\mu F\ cm^{-2}$) in parallel with the transfer resistance, and an inductive impedance at low frequencies characterized by three time constants. The shape of Diagram 1′ obtained during the dissolution of the first deposit is similar to diagrams measured on a bare electrode [5, 6]. One of the two capacitive loops appears in an intermediate frequency range between two inductive loops. The average value of the double-layer capacity calculated from Diagram 1′ is 270 $\mu F\ cm^{-2}$. This value is higher than in [5, 6], thus indicating a possible increase of the electrode roughness. With time, both deposition and dissolution plots change considerably. On passing from Diagrams 1 or 1′ to Diagrams 3 or 3′, the transfer resistances decrease, which can be interpreted as an increase in the electrode area. The diagrams also show some modifications to the frequency characteristic of the loops, thus revealing changes in the electrode kinetics. After three cycles, Diagrams 4, 4′ and 5 have degenerated into a single capacitive line and the low-frequency loops have vanished completely. During deposition, the electrode potential is shifted from − 1.061 to − 1.051 V/SCE, which indicates an overpotential decrease. On the other hand, no change is observed in the electrode potential during dissolution.

For the same thickness of cycled metal, a lower current density yields a faster change in behaviour. For example, at 5 mA cm^{-2}, the impedance diagram obtained after the first cycle is already a capacitive plot similar to Diagram 5 in Fig. 1. Once the solution has been used for these measurements it is no longer possible to reproduce deposition diagrams similar to Diagram 1 in Fig. 1: with a freshly polished electrode, a degenerated impedance spectrum similar to Diagram 5 and a shifted electrode potential (− 1.051 V/SCE) are immediately obtained. In contrast, the dissolution

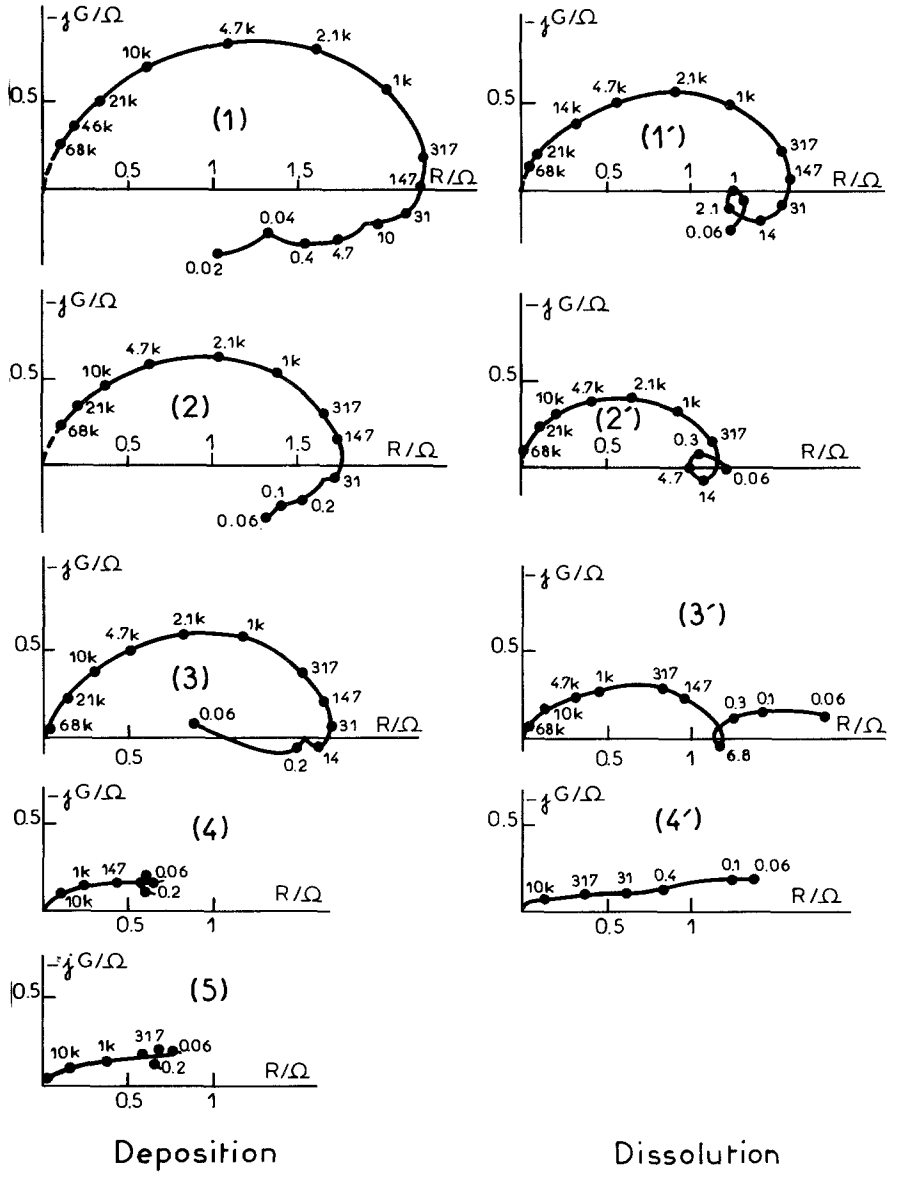

Fig. 1. Complex plane impedance plots (frequency in hertz) obtained during the cycling of a zinc electrode rotated at 2600 r.p.m. Electrolyte: 2.67 M NH_4Cl + 0.72 M $ZnCl_2$, pH = 5.2; current density: 25 mA cm^{-2}; cycle period: 1 hour. Diagrams are numbered as cycles.

diagram obtained on a bare electrode is much less disturbed and similar to Diagram 2'. On the basis of these results it can be concluded that the changes observed in the kinetics of zinc deposition are essentially due to an alteration of the electrolyte.

All these modifications described above can be correlated with a significant change in the electrode morphology. Fig. 2 illustrates the different types of deposit obtained during this study. A compact zinc deposit (Fig. 2a) is observed on a noncycled electrode under the conditions of Diagram 1. After Diagram 5, the electrode seems less compact (Fig. 2b) and partially covered with spongy deposit. On a freshly polished electrode, zinc deposition in the solution already used for the cycles leads to a spongy deposit (Fig. 2c). These SEM photographs confirm an alteration of the electrolyte during the electrode cycling.

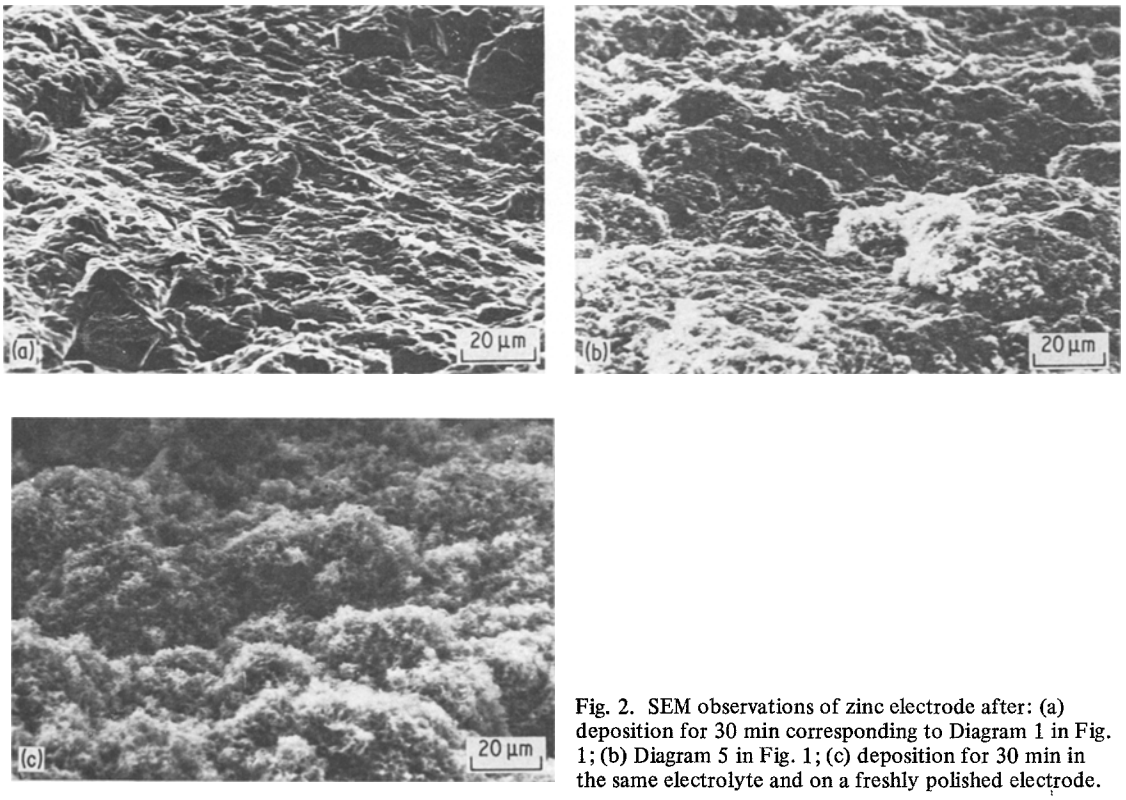

Fig. 2. SEM observations of zinc electrode after: (a) deposition for 30 min corresponding to Diagram 1 in Fig. 1; (b) Diagram 5 in Fig. 1; (c) deposition for 30 min in the same electrolyte and on a freshly polished electrode.

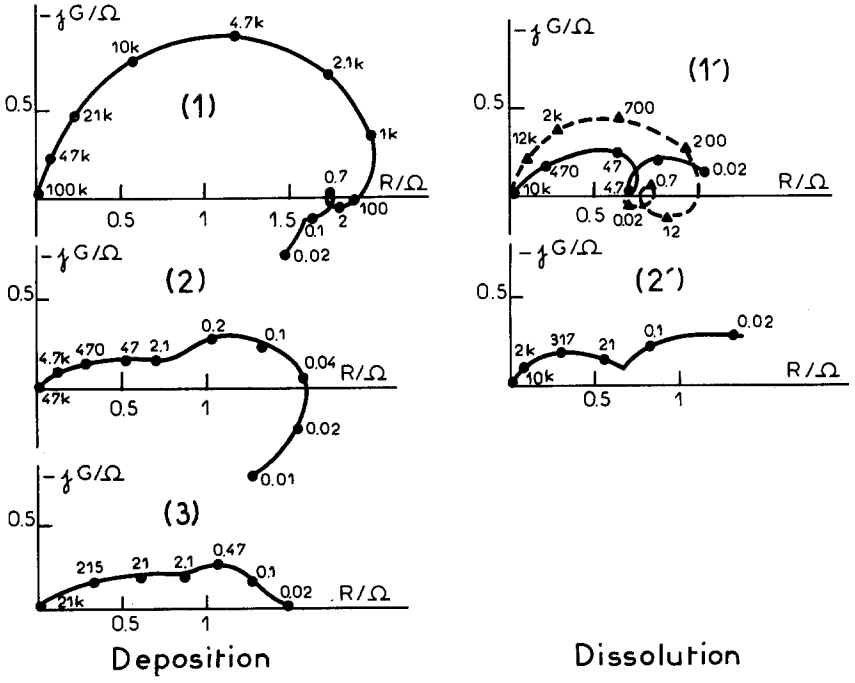

Fig. 3. Complex plane impedance plots (frequency in hertz) obtained during the cycling of a zinc electrode rotated at 2600 r.p.m. Electrolyte: 5 M KOH + 0.5 M ZnO; current density: 25 mA cm^{-2}; cycle period: 1 hour. On Diagram 1' the broken line corresponds to the dissolution of a bare electrode.

3.2. *Zinc electrode cycled in an alkaline zincate solution*

Fig. 3 shows the impedance spectra recorded in the 5 M KOH + 0.5 M ZnO electrolyte when cycling the electrode under the same conditions as in acidic solution (Fig. 1). It appears that the change in electrode surface occurs more rapidly in the alkaline electrolyte than in acidic solution. Only Diagram 1 in Fig. 3, corresponding to the first deposition, is similar to the first diagram of Fig. 1, although there is an additional capacitive loop at frequencies close to 1 Hz, as already reported [1]. Not only does a decrease in the transfer resistance appear on Diagram 2 in Fig. 3, but there is also a change in the shape of the diagram, which indicates modifications to the electrode kinetics. These modifications occur during the first cycle, since the first dissolution (Diagram 1′) is different from that obtained on a bare electrode (broken line). On impedance plots obtained during zinc dissolution, it is noteworthy that the capacity deduced from the high-frequency data is much larger than the double-layer capacity. This leads us to believe that the dissolution of zinc involves a very fast charge transfer.

As in acidic solutions, these changes in impedance diagrams are correlated with a shift of electrode potentials and with modifications to the electrode morphology and they are connected to the continuous change to the electrolyte. Similar variations of morphology with charge–discharge cycles in alkaline solutions [14] have been reported recently.

3.3. *Degeneration of the electrode kinetics during dissolution or deposition*

In an attempt to elucidate the reasons for the deterioration of impedance diagrams with time, we have explored more precisely the time dependence of the zinc electrode during anodic dissolution and cathodic deposition. In both cases, impedance measurements were carried out every hour over a time period of 8 hours. During this time, the study of zinc electrodissolution reveals small variations in the complex-plane spectra. Fig. 4 exemplifies the time dependence of impedance plots obtained in the Leclanché cell electrolyte at a current density of 10 mA cm^{-2}. Comparison of Figs. 4a and 4b shows a slight diminution of the transfer resistance after 8 hours, the characteristic frequencies of all loops being moved towards lower values. In this experiment the electrode potential remains constant. In addition it is worth noting that the application of a new electrode in the same solution leads again to a diagram similar to Fig. 4a. These results prove that dissolution diagrams are not sensitive to a possible change of the electrolyte and that their modifications with time are probably due to the degeneration of the electrode surface.

During zinc electrodeposition, more considerable changes are observed with time. Figs. 5 a–d show the progressive degeneration of the impedance spectra with time for the Leclanché cell electrolyte. At high frequencies similar capacitive loops are obtained in a first approximation, thus revealing an increase in the electrode area. In addition, the modifications to low-frequency loops indicate changes in the reaction rates corresponding to these time constants. After 5 hours, a degeneration of the impedance diagram into a small capacitive loop is seen (Fig. 5d), which resembles Diagram 5 in Fig. 1. It is noticeable that these changes in impedance plots are accompanied by a decrease of cathodic overpotential and by the formation of spongy deposit similar to the

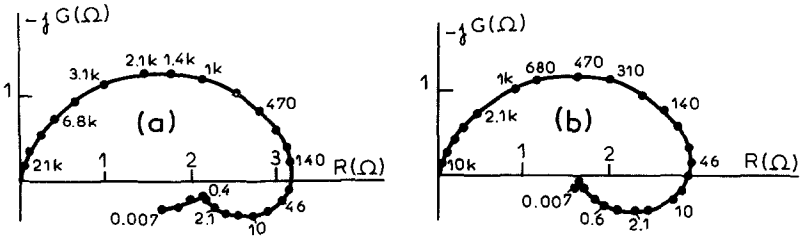

Fig. 4. Variation of complex plane impedance plots (frequency in hertz) with time t during the dissolution of a zinc electrode rotated at 2600 r.p.m. Electrolyte: 2.67 M NH_4Cl + 0.72 M $ZnCl_2$; pH = 5.2; current density: 10 mA cm^{-2}. (a) t = 1 hour, (b) t = 8 hours.

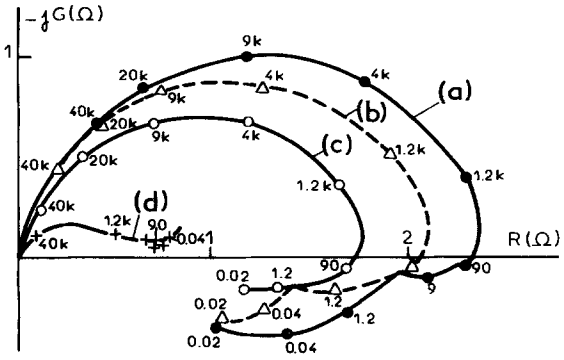

Fig. 5. Variation of complex plane impedance plots (frequency in hertz) with time t during zinc deposition on a zinc electrode rotated at 2600 r.p.m. Electrolyte: 2.67 M NH_4Cl + 0.72 M $ZnCl_2$; pH = 5.2; current density: 25 mA cm^{-2}. (a) t = 0.25 hour, (b) t = 1 hour, (c) t = 2 hours, (d) t = 5 hours.

previous observations during cycling. These modifications are moreover connected to a modification of the electrolyte, since Fig. 5a and a compact deposit cannot be reproduced on a new electrode in the same electrolyte. From a comparison of Fig. 4 and Fig. 5, it can be concluded that zinc deposition is much more sensitive to the electrolyte degeneration than zinc dissolution. Similar results, with a faster evolution, have been observed with the alkaline zincate solution.

In order to determine the origin of the electrolyte degeneration, zinc deposition was also investigated using a platinum counter electrode. Over a time period of 5 hours, the impedance diagrams show only a slight modification: a coalescence of two inductive loops is observed without any change in the transfer resistance. Simultaneously no changes of electrode potential and electrode morphology have been detected. Consequently, it appears that zinc electrocrystallization is disturbed essentially by products emanating from the dissolution of the zinc anode. These products, even in small concentrations, might be able to modify the kinetic behaviour and the morphology of zinc electrodes [15]. During cycles, the zinc electrode being alternately cathode and anode, it is evident that the modifications to impedance spectra will be observed whatever the counter electrode may be.

3.4. *Zinc electrode cycled in the presence of NBu_4Br*

According to Dirkse [11, 12] much interest has been shown in the use of organic compounds in electrochemical power systems with rechargeable zinc electrodes to prevent the dendritic growth of zinc and hence extend the useful cycle life of cells. In the present work, tetrabutylammonium bromide (NBu_4Br), previously reported as an inhibitor of dendritic growth [16, 17], was added to electrolytes, and its influence on the cycle life of zinc electrodes was investigated. Typical diagrams obtained during electrode cycling in Leclanché cell electrolyte with 5×10^{-4} M NBu_4Br are shown in Fig. 6. Each cycle consisted of deposition for 30 min at 25 mA cm^{-2} followed by dissolution for the same time and at the same current density. Diagrams 1 and 1′ in Fig. 6 correspond to the first cycle, Diagrams 19 and 19′ to the 19th cycle and Diagram 24 to the 24th deposition. A comparison of the first diagrams in Fig. 1 and Fig. 6 reveals some changes in electrode kinetics. The value of the double-layer capacitance is decreased by the presence of NBu_4Br from 270 μF cm^{-2} to 120 μF cm^{-2} during the first dissolution. For both deposition and dissolution, NBu_4Br decreases the rate of charge transfer as measured by an increase in the transfer resistance from 2 Ω to 6.5 Ω, and from 1.5 Ω to 3.5 Ω, respectively. Nevertheless, the low values of this resistance indicate that the charge transfer still remains relatively fast. Again, NBu_4Br changes the rate of the interfacial reactions resulting in modifications to the shape of impedance diagrams. In the cathodic domain, the three inductive time constants have coalesced into a single loop. In the anodic domain, a similar impedance diagram is obtained.

The electrode cycling does not induce great changes in the electrode kinetics during zinc deposition and dissolution. Even after 23 cycles, the rates of charge transfer and interfacial reactions

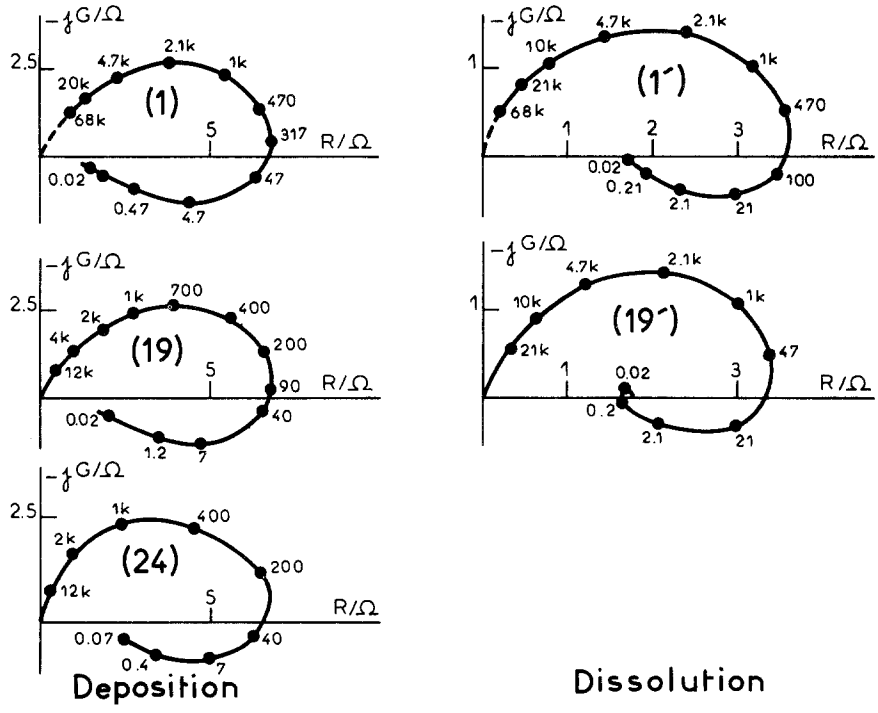

Fig. 6. Complex plane impedance plots (frequency in hertz) obtained during the cycling of a zinc electrode rotated at 2600 r.p.m. Electrolyte: 2.67 M NH_4Cl + 0.72 M $ZnCl_2$ + 5 × 10^{-4} M NBu_4Br; pH = 5.2; current density: 25 mA cm^{-2}; cycle period: 1 hour. Diagrams are numbered as cycles.

are not modified. Only an increase in the double-layer capacitance by a factor of three can be observed on Diagrams 19 and 24 in Fig. 6.

The most significant results obtained in this study of impedance plots are that the presence of NBu_4Br modifies the electrode kinetics and simultaneously extends the cycle life of zinc electrodes. Current–potential curves show that the dissolution as well as the deposition of zinc are inhibited by the addition of NBu_4Br. At a current density of 25 mA cm^{-2}, cathodic and anodic polarizations increase by 35 mV and 25 mV, respectively. It has been observed that this inhibiting effect is not modified with time since the electrode potentials remained constant during the 23 cycles. Also, the deposit remains compact with round protuberances made of numerous crystallites (Fig. 7).

In this study, it is noteworthy that the inhibiting effect of NBu_4Br seems weaker than reported in [3]. In particular, a capacitive loop on the impedance diagrams has disappeared and the increase of cathodic overpotential is less important. A reinforcement of inhibition by potential impurities present in the electrolyte solutions might have been avoided by the additional purification steps, e.g., double distillation of the water, used in our experiments.

The addition of NBu_4Br to the alkaline zincate solutions also modifies the electrode kinetics and improves the cycle life of the zinc electrode. Fig. 8 exemplifies the variation of impedance diagrams with the cycling of the electrode in the alkaline zincate solution of 5 M KOH + 0.5 M ZnO + 5 ×

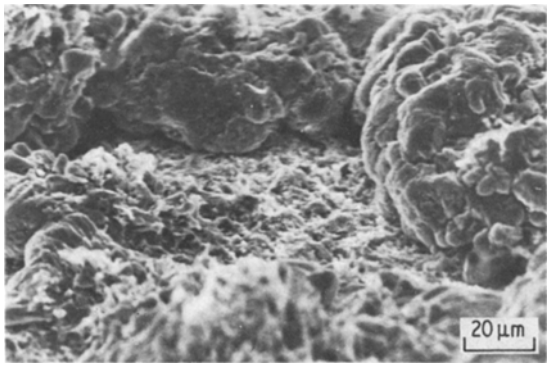

Fig. 7. SEM observation of zinc electrode after Diagram 24 in Fig. 6.

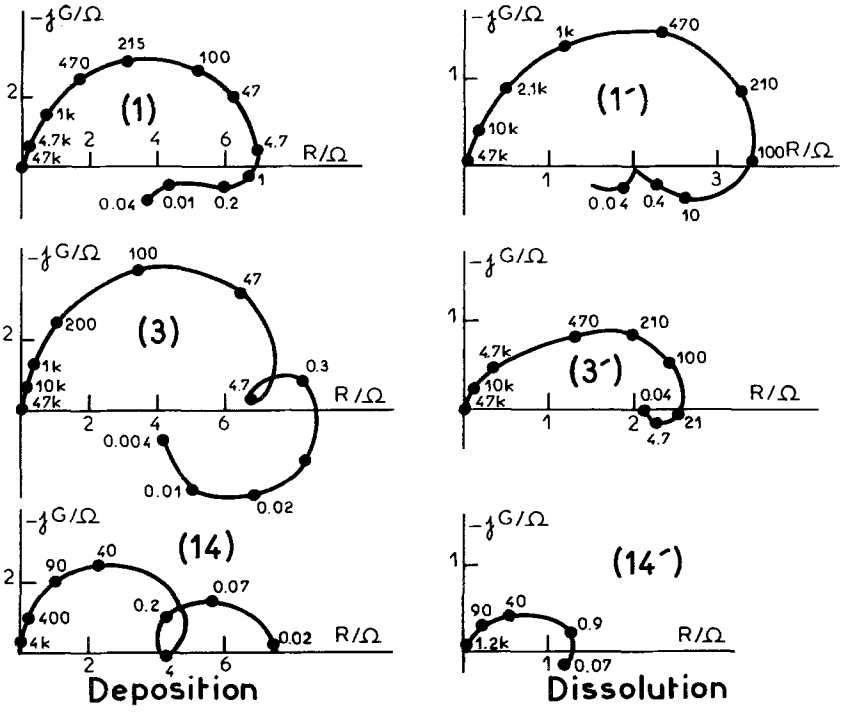

Fig. 8. Complex plane impedance plots (frequency in hertz) obtained during the cycling of a zinc electrode rotated at 2600 r.p.m. Electrolyte: 5 M KOH + 0.5 M ZnO + 5 × 10^{-4} M NBu_4Br; current density: 25 mA cm^{-2}; cycle period: 1 hour. Diagrams are numbered as cycles.

10^{-4} M NBu_4Br. Under the same experimental conditions as for Fig. 6 (current density = 25 mA cm^{-2}, cycle period = 1 hour), the steady state is reached only after a long time and Diagrams 1 and 1′ in Fig. 8, recorded during the first cycle, do not correspond to stationary conditions. After the 2nd cycle, Diagrams 3 and 3′ have been obtained under steady-state conditions. Compared to Fig. 3, Fig. 8 reveals modifications to the interfacial processes involved in the loops obtained at low frequencies. Moreover, it appears that even the capacitive loop apparent at high frequencies for deposition and dissolution in Fig. 8 represents Faradaic processes because the capacity is far too high (about 1000 μF cm^{-2}) to be assigned to the double layer. This result reveals that the charge transfer resistance is probably too low to be attainable during cycling in the presence of NBu_4Br. Impedance plots obtained for the 14th cycle reveal an increase in the electrode area and modifications to the electrode kinetics. At the same time, during the electrode cycling a decrease of polarization is observed over 15 mV for deposition and 6 mV for dissolution. Furthermore the electrode morphology has been altered: a smooth and globular deposit (Fig. 9a) has become irregular with round protuberances made of numerous crystallites (Fig. 9b). All these results obtained in the alkaline electrolyte clearly show that the change in the electrode with time is lessened in the additive-containing electrolyte.

A similar extension of the cycle life has been observed at lower current density, as shown in Fig. 10, where cycles have been performed at 5 mA cm^{-2}, the cycle period being 5 hours so that the thickness of cycled metal remains 21 μm, as in previous experiments. After five cycles, some changes are observed on the impedance plots: in particular all relaxation frequencies are shifted towards lower values with a consequent vanishing of the inductive loop previously existing at the lowest frequencies on Diagrams 1. These changes again suggest modifications of the electrode kinetics. With time a reduction of the impedance diagrams is also observed on Fig. 10, in agreement with the increase of electrode roughness apparent

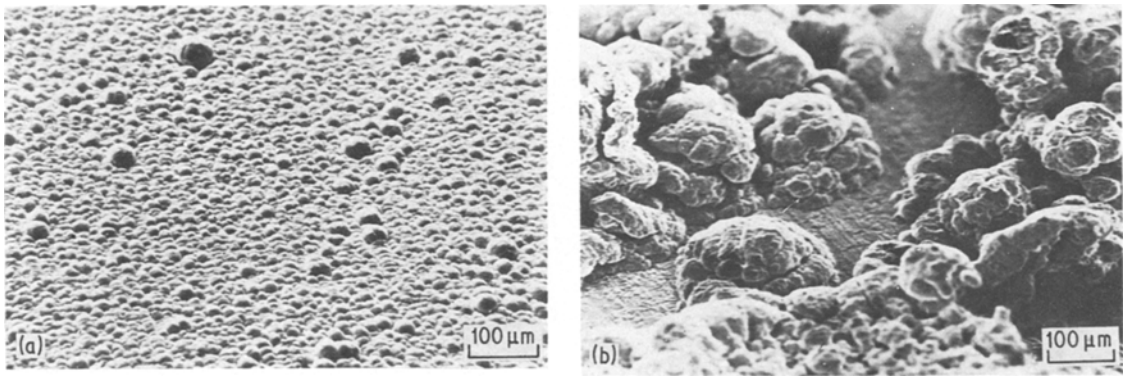

Fig. 9. SEM observation of zinc electrode after: (a) deposition for 30 min corresponding to Diagram 1 in Fig. 8; (b) deposition on the 18th cycle.

on Figs. 11a and b. It is noticeable that between the 10th and 27th cycles, no modification is shown by the impedance plots, thus indicating a stabilization of the electrode kinetics. However, because of the long time (130 hours) necessary to attain the 27th cycle, an evaporation of the electrolyte progressively occurs. On a freshly polished electrode, this modified electrolyte can generate a needle-shaped deposit localized at the electrode centre (Fig. 11c), similar to the deposits obtained in more concentrated electrolytes, for example in the 6 M KOH + 0.5 M ZnO + 5×10^{-4} M NBu_4Br solution. The impedance plots of Fig. 12, which have been obtained during the formation and the dissolution of this non-uniform deposit, exhibit changes in the real and imaginary components

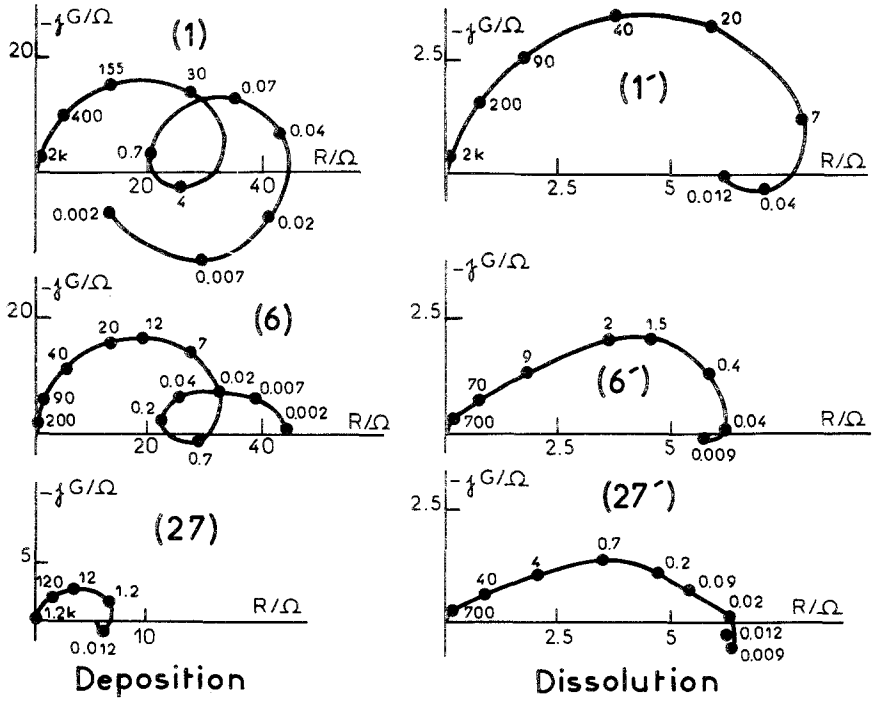

Fig. 10. Complex plane impedance plots (frequency in hertz) obtained during the cycling of a zinc electrode rotated at 2600 r.p.m. Electrolyte: 5 M KOH + 0.5 M ZnO + 5×10^{-4} M NBu_4Br; current density: 5 mA cm^{-2}; cycle period: 5 hours. Diagrams are numbered as cycles.

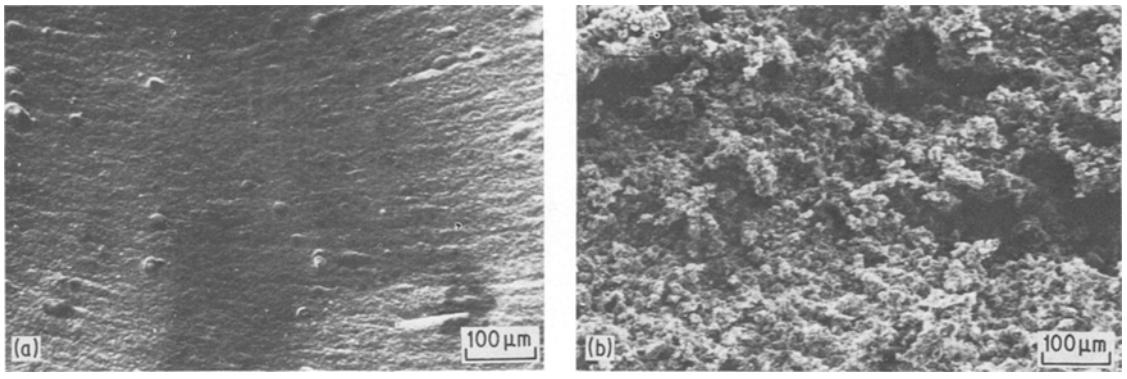

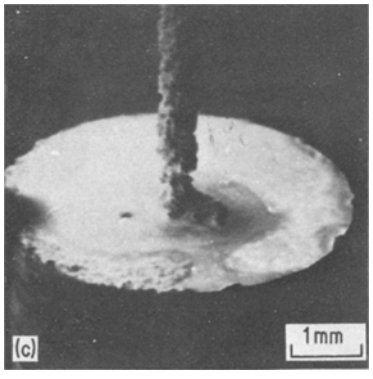

Fig. 11. SEM observation of zinc electrode after: (a) deposition for 2.5 hours, as for Diagram 1 in Fig. 10; (b) the 27th deposition of Fig. 10; (c) deposition for 2.5 hours with the same electrolyte and on a freshly polished electrode, as for Diagram (a) in Fig. 12.

when compared to Diagrams 1 and 1′ in Fig. 10. It is reasonable to think that this electrolyte evaporation could be avoided using a more appropriate cell.

4. Conclusion

The results reported here prove that impedance measurements can be utilized to follow the behaviour of zinc electrodes during their cycling in a Leclanché cell electrolyte as well as in an alkaline zincate solution. The change in the electrode morphology is accompanied by changes in impedance plots thus indicating both an increase in the electrode area and a drift of the electrode kinetics. In additive-free electrolytes it is shown that the electrode degeneration is essentially due to the contamination of electrolytes by dissolution products which strongly affect the interfacial reactions involved in zinc deposition. In acidic and alkaline solutions impedance data confirm that the additive NBu_4Br exerts a beneficial effect on the zinc deposition and dissolution and in this way serves to extend the cycle life of the zinc electrode.

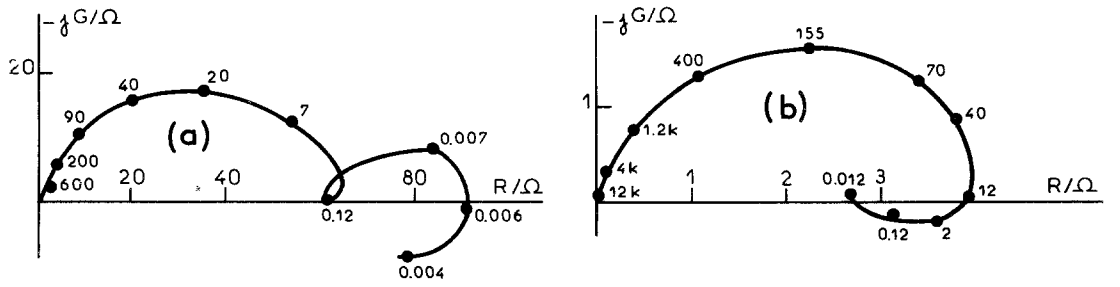

Fig. 12. Complex plane impedance plots (frequency in hertz) obtained on a freshly polished electrode under the same cycling conditions as for Fig. 10 and with the same electrolyte already used for 130 hours. (a) Deposition, (b) dissolution.

Acknowledgements

The work was supported by the ATP CNRS–EDF 'Utilisations Physiques et Chimiques de l'Electricité' as a part of Project 3805. One of us (US) would like to thank the Deutsche Forschungsgemeinschaft for a postdoctoral research fellowship.

References

[1] I. Epelboin, M. Ksouri and R. Wiart, *J. Electrochem. Soc.* **122** (1975) 1206.
[2] *Idem, 12th Faraday Disc. Chem. Soc., Southampton* (1978) p. 115.
[3] J. Bressan and R. Wiart, *J. Appl. Electrochem.* **9** (1979) 43.
[4] *Idem, ibid* **9** (1979) 615.
[5] M. Joussellin and R. Wiart, *Electrochim. Acta* **24** (1979) 891.
[6] C. Cachet and R. Wiart, *J. Electroanal. Chem.* **111** (1980) 235.
[7] *Idem*, to be published.
[8] N. A. Hampson, S. A. G. R. Karunathilaka and R. Leek, *J. Appl. Electrochem.* **10** (1980) 3.
[9] S. A. G. R. Karunathilaka, N. A. Hampson, R. Leek and T. J. Sinclair, *ibid* **10** (1980) 603.
[10] *Idem, ibid* **10** (1980) 799.
[11] T. P. Dirkse and R. Shoemaker, *J. Electrochem. Soc.* **115** (1968) 784.
[12] T. P. Dirkse, *ibid* **115** (1968) 1169.
[13] C. Gabrielli and M. Keddam, *Electrochim. Acta* **19** (1974) 355.
[14] S. Higuchi and S. Takahashi, *Bull. Ind. Res. Instrum., Osaka, Japan* **30** (1979) 219.
[15] D. J. Mackinnon, J. M. Brannen and R. C. Kerby, *J. Appl. Electrochem.* **9** (1979) 71.
[16] F. Mansfeld and S. Gilman, *J. Electrochem. Soc.* **117** (1970) 1154.
[17] J. W. Diggle and A. Damjanovic, *ibid* **119** (1972) 1649.